tvst

Glaucoma

Development of a Novel Valve-Controlled Drug-Elutable Microstent for Microinvasive Glaucoma Surgery: In Vitro and Preclinical In Vivo Studies

Stefan Siewert[1,*], Sabine Kischkel[2,*], Andreas Brietzke[2], Ludmila Kinzel[3], Tobias Lindner[4], Ulf Hinze[5,6], Boris Chichkov[5,6], Wolfram Schmidt[2], Michael Stiehm[1], Niels Grabow[2], Rudolf F. Guthoff[3], Klaus-Peter Schmitz[1,2], and Thomas Stahnke[1,3]

[1] Institute for ImplantTechnology and Biomaterials e.V., Rostock-Warnemünde, Germany
[2] Institute for Biomedical Engineering, Rostock University Medical Center, Rostock, Germany
[3] Department of Ophthalmology, Rostock University Medical Center, Rostock, Germany
[4] Core Facility Multimodal Small Animal Imaging, Rostock University Medical Center, Rostock, Germany
[5] Institute of Quantum Optics, Faculty of Mathematics and Physics, Leibniz University Hannover, Hannover, Germany
[6] Laser nanoFab GmbH, Garbsen, Germany

Correspondence: Stefan Siewert, Institute for ImplantTechnology and Biomaterials e.V., Friedrich-Barnewitz-Straße 4, 18119 Rostock-Warnemünde, Germany.
e-mail: stefan.siewert@iib-ev.de

Received: April 9, 2022
Accepted: January 24, 2023
Published: March 1, 2023

Keywords: microinvasive glaucoma surgery; MIGS; microstent; valve-controlled; drug-elutable; glaucoma drainage device; GDD

Citation: Siewert S, Kischkel S, Brietzke A, Kinzel L, Lindner T, Hinze U, Chichkov B, Schmidt W, Stiehm M, Grabow N, Guthoff RF, Schmitz KP, Stahnke T. Development of a novel valve-controlled drug-elutable microstent for microinvasive glaucoma surgery: In vitro and preclinical in vivo studies. Transl Vis Sci Technol. 2023;12(3):4, https://doi.org/10.1167/tvst.12.3.4

Purpose: Microinvasive glaucoma surgery (MIGS) has become an important treatment approach for primary open-angle glaucoma, although the safe and long-term effective lowering of intraocular pressure with currently available implants for MIGS is not yet achieved to a satisfactory extent. The study focusses on the development and in vitro and in vivo testing of a novel microstent for MIGS.

Methods: A silicone elastomer-based microstent was developed. Implants were manufactured using dip coating, fs-laser cutting, and spray coating. Within the current study no antifibrotic drug was loaded into the device. Sterilized microstents were analyzed in vitro regarding pressure–flow characteristics and biocompatibility. Six New Zealand white rabbits were implanted with a microstent draining the aqueous humor from the anterior chamber into the subconjunctival space. Drainage efficacy was evaluated using oculopressure tonometry as a transient glaucoma model. Noninvasive imaging was performed.

Results: Microstents were manufactured successfully and characterized in vitro. Implantation in vivo was successful for four animals with additional device fixation. Without additional fixation, dislocation of microstents was found in two animals. Safe and effective intraocular pressure reduction was observed for the four eyes with correctly implanted microstent during the 6-month trial period.

Conclusions: The described microstent represents an innovative treatment approach for MIGS. The incorporation of a selectively antifibrotic drug into the microstent drug-elutable coating will be addressed in future investigations.

Translational Relevance: The current preclinical study successfully provided proof of concept for our microstent for MIGS which is suitable for safe and effective intraocular pressure reduction and offers promising perspectives for the clinical management of glaucoma.

Introduction

Glaucoma represents a widespread disease and a main cause of vision impairment and irreversible blindness worldwide.[1] Lowering of the intraocular pressure (IOP) to a patient-specific target value is the basis of all therapeutic approaches to prevent further progression of structural damage and functional visual deficiencies.[2]

Topical application of medication serves as the primary treatment option for patients suffering from primary open angle glaucoma, the most prevalent form.[3,4] Laser trabeculoplasty as an alternative safe and effective first-line treatment or surgical procedures such as trabeculectomy are also used in case of insufficient IOP reduction. Since the introduction of glaucoma drainage devices (GDD) in 1969 by Molteno,[5] these implants are used increasingly in glaucoma surgery. Conventional GDD in a tube and plate design drain aqueous humor from the anterior chamber of the eye into the subconjunctival space using a silicone drainage tube. A polymeric plate that is partly equipped with a valve mechanism stretches out the outflow area. Commercially available devices of this type include Molteno (Molteno Ophthalmic Ltd., Dunedin, New Zealand), Baerveldt (Abbott Medical Optics Inc., Irvine, CA), or Ahmed (New World Medical Inc., Rancho Cucamonga, CA).[5,6] Currently, implants for microinvasive glaucoma surgery (MIGS) are increasingly used as a promising alternative to conventional GDD. MIGS devices are implanted by means of a minimally invasive approach ab interno using a clear corneal incision, exclusively. Therefore, ocular traumas, that is, surgically induced lesions to the eye caused by the implantation process, as well as postoperative complication rates, are decreased compared with conventional surgery and conventional GDD.[2,7] MIGS devices such as iStent or iStent inject (Glaukos Inc., San Clemente, CA), CyPass microstent (Alcon Inc., Fort Worth, TX), which was recently withdrawn from the market because of severe side effects, or XEN gel stent (Allergan PLC, Dublin, Ireland) enable a drainage of aqueous humor from the anterior chamber of the eye into Schlemm's canal and the suprachoroidal and subconjunctival space, respectively.

Early postoperative hypotony is known as a major limitation of GDD and MIGS devices.[7–13] Fibrosis-induced occlusion and consecutive implant failure represents a second limitation of current generation devices.[14–17] As a further complication, safety issues with regard to corneal endothelial cell loss have been reported, like in case of the CyPass microstent.[18]

As an innovative treatment approach, our group focusses on the development of a minimally invasive implantable valve-controlled microstent for MIGS. Our unique patent-registered micromechanical valve mechanism for safe IOP regulation has been described previously.[19] The drug-elutable coating of the device can be loaded with antifibrotic drugs, such as pirfenidone (PFD), which successfully found its way in ophthalmological applications.[20,21,22] Furthermore, our new therapy concept is based on a minimally invasive implantation procedure.[23] The current work focuses on the development, design, and testing of our valve-controlled drug-elutable microstent for MIGS. The soft polymeric device is designed for drainage of aqueous humor from the anterior chamber of the eye into subconjunctival space. Microstent prototypes were manufactured in laboratory scale by means of dip coating, fs-laser cutting, and spray coating. Within the current study, no antifibrotic drug was loaded into the drug-elutable coating. Further processing includes sterilization by means of ethylene oxide. In vitro testing was conducted in accordance to ANSI Z80.27-2014 and the 2015 Guidance for Industry and Food and Drug Administration Staff "Premarket Studies of Implantable Minimally Invasive Glaucoma Surgical (MIGS) Devices" (2015 FDA Guidance). Biocompatibility of microstent material was analyzed using human primary fibroblasts.[24] Safety and efficacy of fully processed minimally invasive implanted microstents were analyzed in rabbits in vivo for a trial period of 6 months. The primary aim of the current work was to evaluate our in-house developed microstent for the treatment of glaucoma in vitro and in vivo, which avoids crucial disadvantages of glaucoma implants already on the market by decreasing side effects to guarantee long-term functionality of the implant.

Methods

Concept and Design of Microstents

The concept of our microstent for MIGS has been described previously (Fig. 1).[19,22] The flexible tubular microstent is composed of a polycarbonate-based silicone elastomer and shunts the anterior chamber of the eye to the subconjunctival space. According to Hagen Poiseuille's law for stationary laminar flow of a Newtonian fluid in a pipe with a circular cross-section, a volume flow of approximately 680 µL min^{-1} would be expected for a simple tube with the dimensions of our microstent. Therefore, for the prevention of ocular hypotony, a pressure-controlled valve is located in the inflow area of the device, while the tubing inflow lumen is sealed.[19] The outflow area of the device includes a drug-elutable coating for the prevention of fibrosis, presupposing that an antifibrotic agent is incorporated into the coating.[21,22] However, within the current work we focused on a microstent control group with no antifibrotic drug incorporated into the coating. Irrespective of this, within the current study the drug-elutable coating was produced in the same way as planned in future test groups with incorporated antifibrotic drugs.

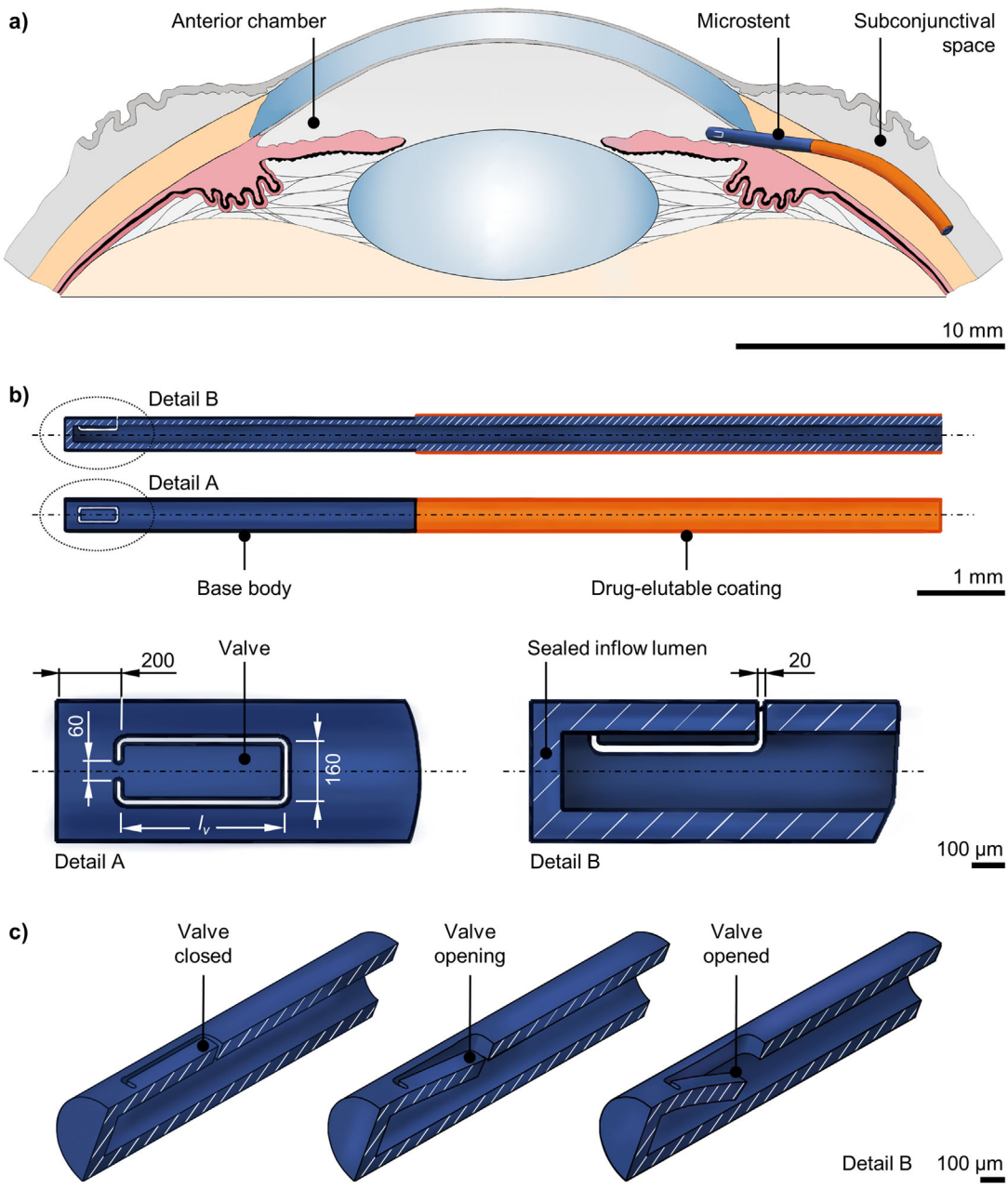

Figure 1. Concept of a minimally invasive implantable valve-controlled drug-elutable microstent for glaucoma therapy. (a) Schematic representation of the position of the microstent for drainage of aqueous humor from the anterior chamber of the eye into the subconjunctival space. (b) Cross-sectional and top view of microstent geometry: tubular base body (inner diameter 200 µm, outer diameter 360 µm, length 10 mm) in blue with sealed inflow lumen and pressure-controlled valve mechanism in the inflow area and drug-elutable coating (*orange*) in the outflow area (length of drug-elutable coating 6 mm). Valve dimensions in µm. (c) Valve configuration in cross-sectional isometric view: valve closed and minor drainage at a low pressure difference between the anterior chamber of the eye and the subconjunctival space (*left*), valve opening and minor drainage at a physiological pressure difference of 10 mm Hg (*middle*) and valve opened and maximum drainage at a high pressure difference (*right*).

Geometrical dimensioning of the pressure controlled valve was conducted using a finite element analysis (FEA, ABAQUS 2020, Dassault Systèmes SE, Vélizy-Villacoublay, France) as methodically described previously.[19] Considering a physiological pressure difference between the anterior chamber of the eye and the subconjunctival space, a valve opening and a closing pressure of 10 mm Hg was aspired. For the adjustment of the valve characteristics, geometric valve length was varied in the range of 300 µm $\leq l_v \leq$ 700 µm (Fig. 1). Material characteristics as input value for FEA were determined by means of tensile testing

(BZ 2.5/TN1S, Zwick GmbH & Co. KG, Ulm, Germany) of polymeric cast film samples with a thickness of 61 ± 8 µm ($n = 3$) in water at 35 ± 2°C. Hyperelastic material behavior was implemented in FEA using a polynomial strain energy potential of second order and a Poisson ratio of $\nu = 0.45$.

Manufacturing of Microstents, Morphological Characterization, and Pressure–Flow Characterization In Vitro

The manufacturing of the microstents was based on dip coating (KSV NIMA Dip Coater, Biolin Scientific Holding AB, Stockholm, Sweden) of tubular polymeric base bodies (inner diameter of 200 µm, outer diameter of 360 µm, length $l = 10$ mm) using stainless steel 200-µm dipping mandrels. A chloroform based 4% (w/v) solution of polycarbonate based silicone elastomer was used.[23] Drying was conducted in vacuum for four days at 40°C. Dipping mandrels were removed and sealing of microstent inflow lumen was conducted by subsequent dipping of base bodies into the previously described polymer solution. Diameter measurement of base bodies was performed using a biaxial laser scanner (ODAC 32 XY, Zumbach Electronic AG, Orpund, Switzerland). For manufacturing of flap valve mechanisms an fs-laser setup was used as described previously.[19]

The design of the drug-elutable coating of our microstent for MIGS refers to Jung and Park.[20,22] Within the current work, a control group with a coating without the antifibrotic drug PFD incorporated is described. Therefore, microstents were spray coated with an aspired mass of $m = 89$ µg of the above described polymer solution.[22] The mass of the coated and dried microstents was measured using an ultramicrobalance (XP6U, Mettler-Toledo International, Inc., Greifensee, Switzerland). Microstent sterilization was performed using ethylene oxide.

Microstent prototypes were analyzed by means of scanning electron microscopy (Quattro S, Thermo Fisher Scientific, Waltham, MA) in low vacuum mode without using conductive coating. The volumetric flow rate through the microstent as a function of the pressure difference was measured in vitro according to ANSI Z80.27-2014 and the 2015 US Food and Drug Administration guidance. Pressure–flow characterization was conducted using an in-house developed test setup (Supplementary Material S1).[19] Microstents were pressurized in the range of 0 mm Hg $\leq \Delta p \leq$ 21 mm Hg in steps of 1 mm Hg and the volumetric flow rate was measured. The analysis was conducted using ultrapure water at 35 ± 2°C.

Preclinical Testing of Microstents In Vivo

Animal Model

Animal experiments were approved by the governmental ethical board for animal research (Landesamt für Landwirtschaft, Lebensmittelsicherheit und Fischerei, Mecklenburg-Vorpommern, Germany; No.7221.3-1-005/18) and carried out in accordance with the EU-directive 2010/63/EU. The authors complied with the ARRIVE guidelines. Six healthy adult female New Zealand white rabbits (Charles River, Sulzfeld, Germany) weighing 3.03 ± 0.17 kg at the beginning of experiments were included. The animals housed in standard cages at 18 ± 3°C under a 12-hour light/dark cycle, with free access to water and a standard diet, without fasting on experimental days.

Surgical Procedure

The surgical procedure was tested extensively ex vivo, leading to a complete implantation within 20 minutes. Briefly, microstents were inserted through a temporoinferior paracentesis using an in-house developed applicator which was described in detail elsewhere.[23] The applicator device is based on a 22G × $1\frac{1}{2}$" cannulated needle (Sterican, B. Braun Melsungen AG, Melsungen, Germany) attached to a handgrip including the release mechanism for the microstent, loaded inside the tip of the cannulated needle.[22,23] The design of the injector device allows the use of a fresh sterile cannulated needle after each implantation.

The surgical implantation process is schematically demonstrated in Figure 2. The cannulated needle of the applicator penetrated the iridocorneal angle and the sclera (Fig. 2c). For microstent release under the conjunctiva, the applicator device enables the microstent to be held in position and the cannula to be withdrawn in the process, leaving the inflow ending in the anterior chamber (Fig. 2e), ensuring drainage into the subconjunctival space. Microsurgical access via the conjunctiva was created and the microstents were mattress suture fixated onto the sclera (Fig. 2f) using 10-0 nylon (MPZ671, Ethicon, Johnson & Johnson Medical GmbH, Norderstedt, Germany) to prevent dislocation.

For in vivo implantations, animals were sedated using a subcutaneous injection of 50 mg kg^{-1} ketamine 10% (Belapharm GmbH & Co. KG, Vechta, Germany) and 5 mg kg^{-1} xylazine 2% (Rompun, Bayer Vital GmbH, Leverkusen, Germany). Animals were implanted with one microstent into the right (treated) eye. The left (untreated) eye remained without an implant and served as a control. All implantations were performed by the same surgeon. After stent implantation, antibiotic eye drops (Dexa-Gentamicin,

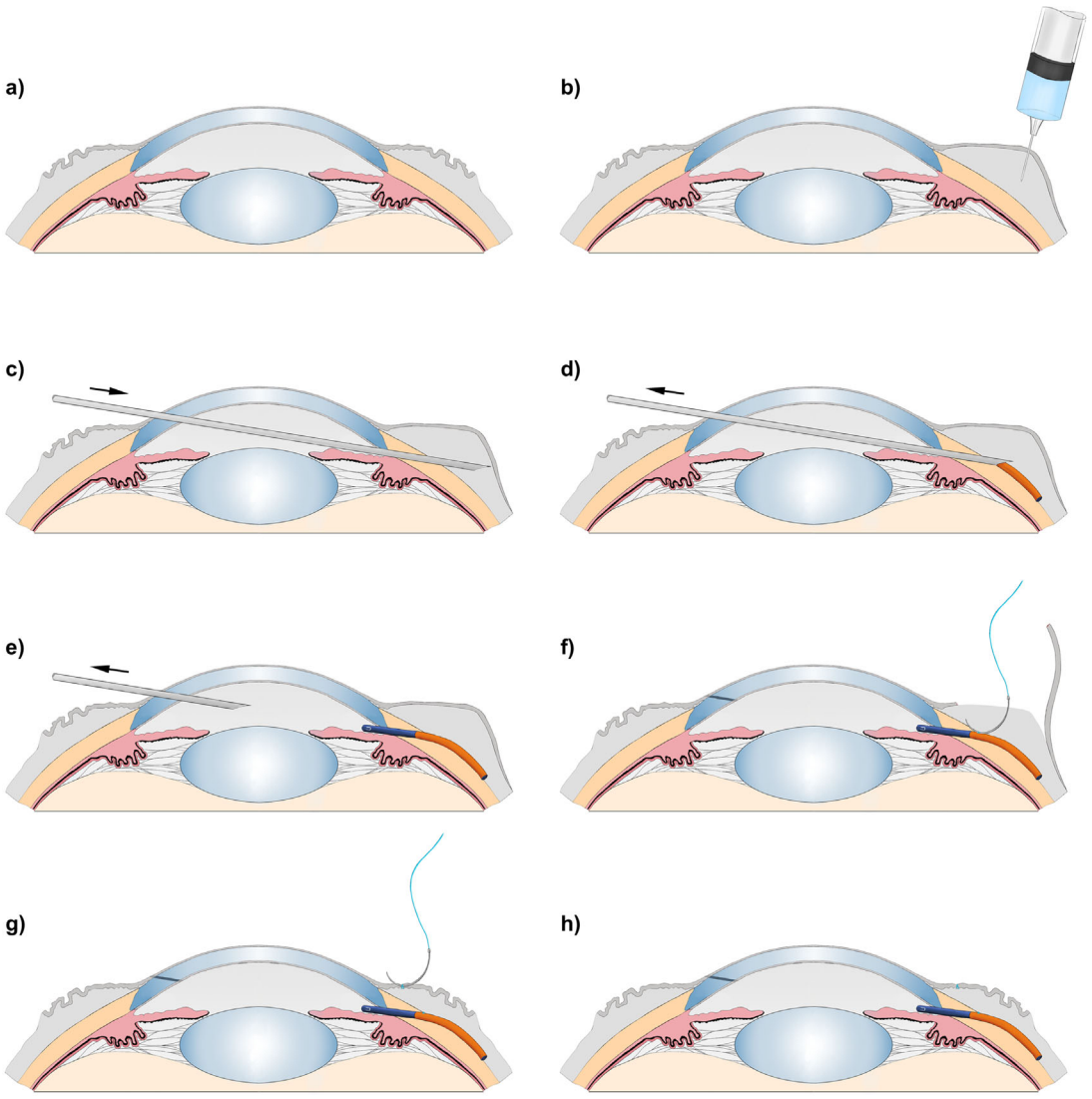

Figure 2. Schematic drawing of minimally invasive microstent implantation into the subconjunctival space. (a) Preoperative situation. (b) Expansion of subconjunctival space by NaCl injection using a 27G cannula. (c) Clear corneal paracentesis and insertion of the microstent applicator device. (d, e) Release of the microstent. (f) Microsurgical access via the conjunctiva and suture fixation of microstent onto the sclera. (g) Suture fixation of conjunctiva. (h) Postoperative situation.

Ursapharm GmbH, Saarbrücken, Germany) were administered postsurgically to the treated eye three times a day for 5 days.

Noninvasive Measurement of IOP

A rebound tonometer (TA01, Icare Finland Oy, Vantaa, Finland) was used for noninvasive measurement of IOP. To adapt measured IOP values p_{Icare} considering rabbit cornea stiffness, recorded values were corrected by a linear function as described elsewhere.[25] IOP measurement was conducted once per week, 4 weeks before and 21 weeks after surgery in both eyes. IOP values represent an arithmetic mean of six single measurements.

Oculopressure Tonometry (OPT) as a Transient Glaucoma Model

For functionality testing of the implanted microstents, OPT was applied as an existing method to quantify retinal and ciliary blood pressures as well as perfusion pressures in humans.[26,27] A suction cup oculopressor (Fa. B. Boucke, Medizin-Elektronik, Tübingen, Germany) approved in human medicine, consisting of a vacuum pump that is connected to the eyeball by a flexible tube, was used. The suction cup was adjusted to the anatomy of the rabbit eye as described elsewhere.[28] Briefly, the suction cup oculopressor was used to increase the IOP about 40 mm Hg during an examination period of eight minutes. Before IOP increase using a suction cup oculopressor, the

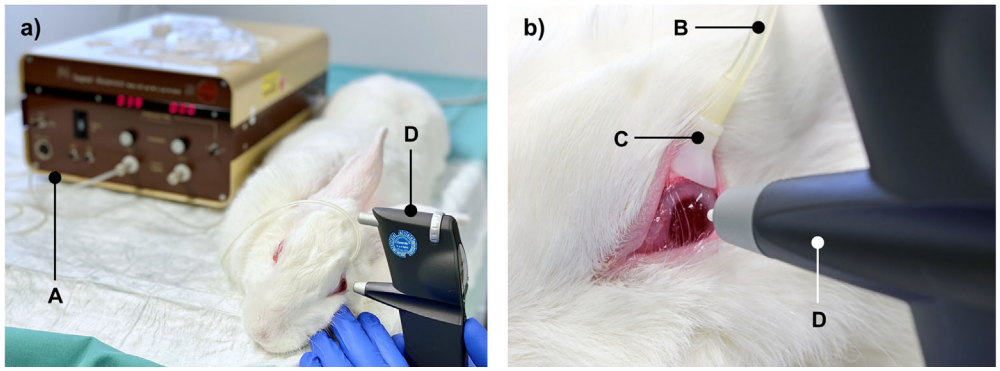

Figure 3. OPT as transient in vivo glaucoma model. (a) OPT measurement setup for the analysis of New Zealand white rabbit's eyes. (b) Detail of the analyzed eye during OPT. Components of OPT measurement setup: suction cup oculopressor (SCOP) (A), hose fitting to SCOP (B), suction cup on eyeball (C) and rebound tonometer (D).

initial baseline IOP was measured. During OPT, the IOP was measured using the rebound tonometer (Fig. 3). To record pressure decay during OPT, the IOP was measured every minute. Finally, IOP was recorded eight minutes after termination of OPT. Upon completion of a series of measurements a moisturizing gel (Vidisic; Bausch & Lomb GmbH, Berlin, Germany) was applied to the eyes. In total, OPT was performed under general anesthesia as already described above, at 4 weeks postoperatively and subsequently every 4 weeks until the end of the study.

Noninvasive Imaging by Optical Coherence Tomography (OCT) and Magnetic Resonance Imaging (MRI)

All imaging was performed under general anesthesia as already described above. OCT (SOCT Copernicus; OPTOPOL Technology S.A., Zawiercie, Poland; wavelength 840 nm, axial resolution 6 µm, and transversal resolution of 12–18 µm) was performed bilaterally on all rabbit eyes. To visualize the iridocorneal angle, including the inflow area of the implanted microstent in case of operated eyes, the animals were positioned upright in front of the device and the eye was opened by a lid speculum for OCT examination. OCT was carried out 2 weeks as well as 4 weeks after surgery and then subsequently every 4 weeks until the end of the study to evaluate the correct position of the implants and to detect implant dislocations at an early stage.

MRI of the microstents was performed with an ultrahigh field small animal MR scanner (7 Tesla, BioSpec 70/30 USR, gradient: BGA 20S, gradient strength: 200 mT/m, Bruker BioSpin MRI GmbH, Bremen, Germany) equipped with a 152-mm (inner diameter) volume resonator in transmit-only mode, and a 2 × 2 receive-only surface coil in receive mode (both Bruker). Animal eyes were imaged in coronal and sagittal slice orientation using a T2-weighted Turbo-RARE sequence (TE/TR = 35/4000 ms, rare factor = 8, averages = 1, field of view = 20 × 18.7 mm, matrix = 133 × 125, slice thickness = 1.0 mm, in-plane resolution = 150 µm × 150 µm).

For the MRI measurement, the breathing rate of the rabbits was monitored (Model 1030, SA Instruments Inc., Stony Brook, NY) during the scans. To prevent eyes from drying Vidisic eye gel (Bausch & Lomb Inc., Rochester, NY) was used and the lids were carefully shut. The surface coil was placed proximal to the closed eye. The first MRI was conducted 4 weeks after surgery and subsequently every 4 weeks until the end of the study.

Statistical Analyses

In general, data from the in vitro and in vivo experiments are presented as mean ± standard deviation (SD). In the in vivo experiments, the total number of six tested New Zealand white rabbits was divided into two groups of $n = 4$ and $n = 2$ animals. Because of the small number of animals, no statistical comparisons were made for the in vivo experiments.

Results

Developed Microstents: Morphological Characterization and Pressure–Flow Characterization In Vitro

Microstent base material shows a stress-strain behavior typical for elastomers, characterized by an elastic modulus $E = (4.2 \pm 0.4)$ N mm^{-2}, a tensile strength $\sigma_m = (57.6 \pm 9.3)$ N mm^{-2}, and an elongation at break of $\varepsilon_B = (950.5 \pm 78.7)\%$, $n = 3$,

respectively. The influence of the geometrical valve length on the valve opening pressure was investigated as part of a parameter study by means of FEA. Using a valve length of $l_v = 410$ µm, the desired valve opening pressure of 10 mm Hg, corresponding with the physiological pressure difference between the anterior chamber of the eye and the subconjunctival space, is achieved (Fig. 4a).

Manufacturing of microstent base bodies yields a reproducible inner diameter of 200 ± 0 µm and an outer diameter of 359 ± 7 µm ($n = 12$). The targeted valve dimensions, according to the FEA, were achieved by fs-laser manufacturing. Coating of microstents yields a smooth surface and a coating mass of $m = 93 \pm 11$ µg ($n = 12$) after drying. Scanning electron micrographs of a representative valve-controlled microstent prototype are shown in Fig. 4b.

A representative pressure–flow curve resulting from fluid mechanic characterization of microstent prototypes is shown in Figure 4c. Valve opening and closing pressures of $p_o = 10 \pm 2$ mm Hg and $p_c = 11 \pm 1$ mm Hg were determined at the intersection of the tangents applied to the pressure–flow curves ($n = 4$), respectively.

Preclinical Testing of Microstents In Vivo

Microstent Implantation

Before preclinical testing of microstents in vivo, biocompatibility of microstent material was proven (see Supplementary Material S2). Valve-controlled microstents were implanted into the subconjunctival space using a scleral fixation as described in Figure 2 ($n = 4$; group A, stent positionally

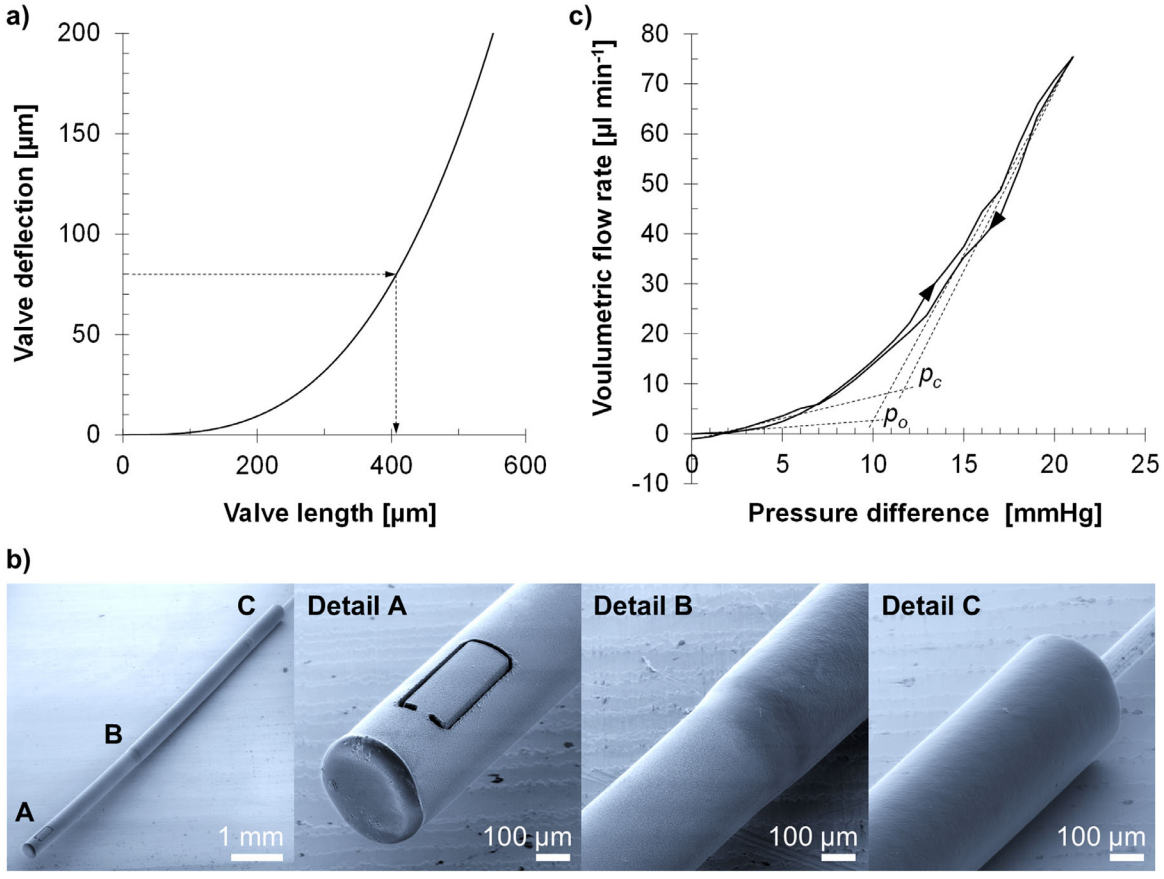

Figure 4. (a) Results of FEA parameter study for geometrical dimensioning of pressure controlled valve. Influence of the valve length on the valve deflection at the aspired valve opening pressure of 10 mm Hg. Considering a wall thickness of 80 µm, a minimum valve deflection of 80 µm is necessary for valve opening. Therefore, a valve length of 410 µm is needed. (b) Scanning electron microscopy of a finally processed microstent prototype: sealed inflow lumen and valve in the inflow area (*Detail A*), transition between uncoated (*Detail B*) and coated area (*Detail C*). (c) Exemplary pressure–flow curve of a valve-controlled microstent measured at 35 ± 2°C using ultrapure water as flow medium. Pressurization and depressurization in the range of 0 mm Hg $\leq \Delta p \leq$ 21 mm Hg indicated by arrowheads. Determination of valve opening pressure p_o and valve closing pressure p_c at the intersection of the tangents applied to the pressure–flow curves, respectively.

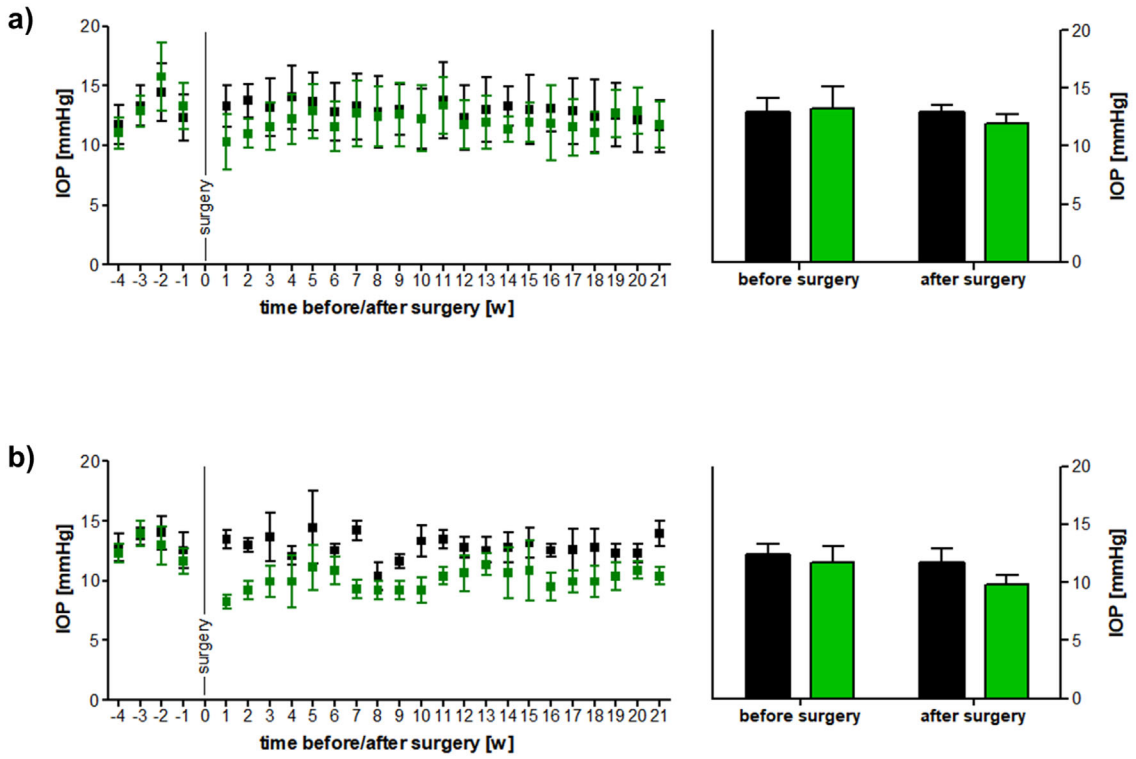

Figure 5. IOP values (mean ± SD; $n = 6$ recordings per animal and point in time) of right treated eyes (*green square/green bar*) and left untreated control eyes (*black square/black bar*) during the trial period of 6 months (*left*) and summarized before and after surgery (*right*). (a) Group A: microstents positionally stable ($n = 4$ rabbits) and (b) group B: microstents migrated/dislocated ($n = 2$ rabbits).

stable) and without scleral fixation ($n = 2$; group B, stent migrated/dislocated). A step-by-step intraoperative photo documentation is given in Supplementary Material S3.

All rabbits showed chemosis of the conjunctiva and mild corneal edema 24 hours after implantation. A prominently formed filtering bleb and swollen upper eyelid was observed to recede after 48 hours. On postoperative day 5, the conjunctiva was irritation free, the cornea was smooth and clear, and the filtering bleb flat. The initially implanted two microstents (group B) were not fixated to the sclera and migrated into the anterior chamber without any signs of infection. Four consecutively implanted microstents (group A) were suture fixated onto the sclera to prevent dislocation. No pathological findings were reported for the untreated left control eyes in all animals during the whole trial period of 6 months. All animals survived until the end of the study. No wound associated complications were observed. After a 6-month trial period animals reached a body weight of 3.95 ± 0.32 kg ($n = 6$).

IOP Monitoring

Before surgery, comparable IOP values were measured in left eyes ($p_{left} = 13.12 \pm 0.93$ mm Hg) and right eyes ($p_{right} = 12.97 \pm 1.46$ mm Hg) of all animals ($n = 6$). After surgery, the IOP in the left (untreated) eyes (control eyes) stays constantly on the preoperative level in all animals ($p_{left} = 12.91 \pm 0.77$ mm Hg; $n = 6$). Therefore, any IOP change in the right (treated) eyes is associated with the microstent implantation. Comparing IOP values before and after surgery, a percentage difference in the left (untreated) eyes (control eyes) of 0.1% (group A; $n = 4$) and 3.1% (group B; $n = 2$) was found. In the right (treated) eyes, a percentage difference before and after surgery of 9.5% (group A; $n = 4$) and 20.8% (group B; $n = 2$) was found (Fig. 5).

Microstent Performance Under Transient Glaucoma Conditions

Before OPT, the baseline IOP was measured on the anesthetized rabbits. In general, IOP values of anesthetized rabbits are on average 3.56 ± 1.79 mm Hg lower compared with IOP values measured on rabbits awake. During OPT, a greater IOP increase was found in the left (untreated) eyes (control eyes) compared with the right (treated) eyes. During 8 minutes of OPT, IOP values decreased continuously for untreated control eyes (left eyes) and right (treated) eyes. After OPT, the baseline IOP in both eyes was reached within 8 minutes.

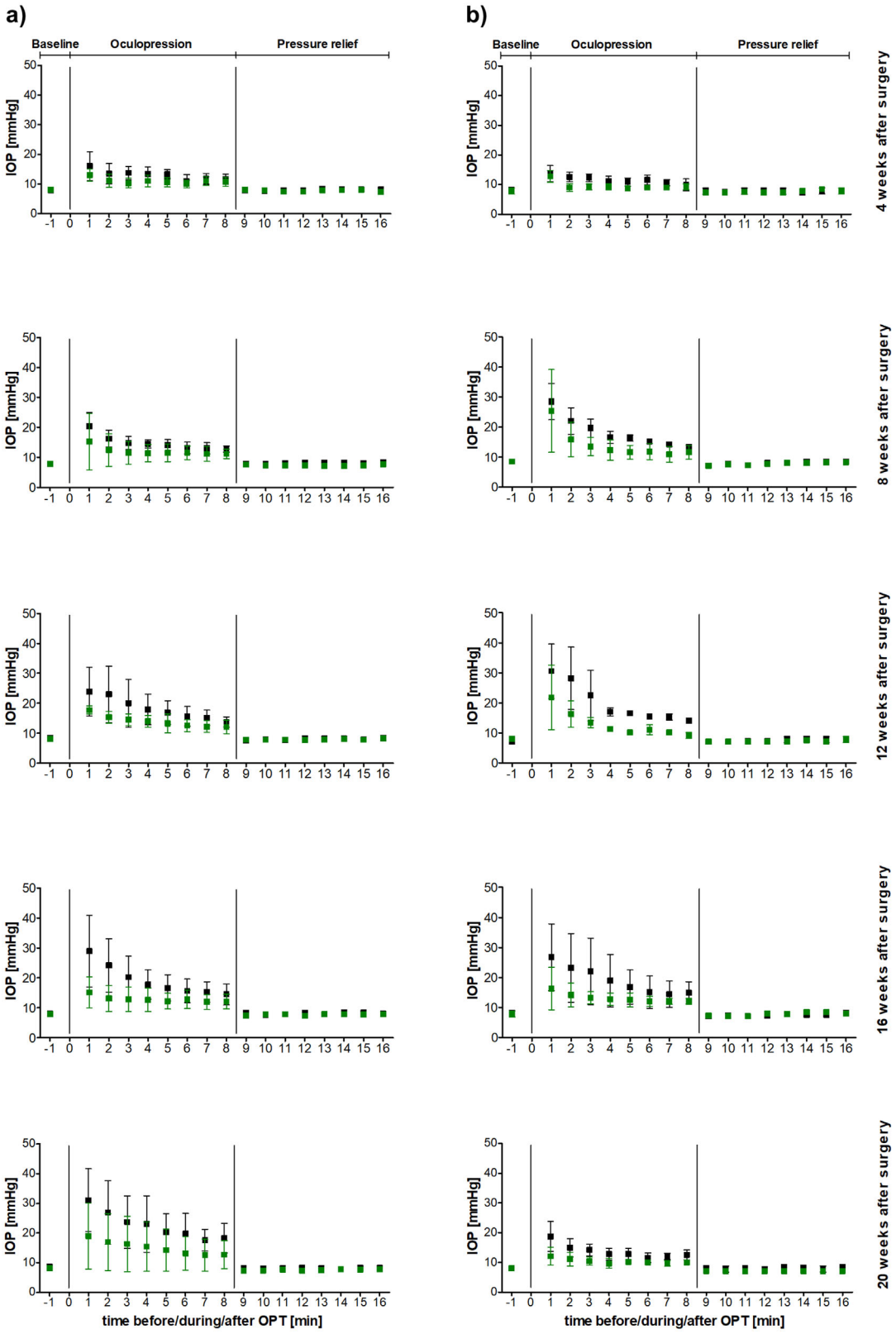

Figure 6. IOP values (mean ± SD; $n = 6$ recordings per animal and point in time) of right treated eyes (*green square*) and left untreated control eyes (*black square*) during the postoperative trial period (points in time: 4, 8, 12, 16, and 20 weeks postoperatively). (a) Group A: microstents positionally stable ($n = 4$ rabbits) and (b) group B: microstents migrated/dislocated ($n = 2$ rabbits).

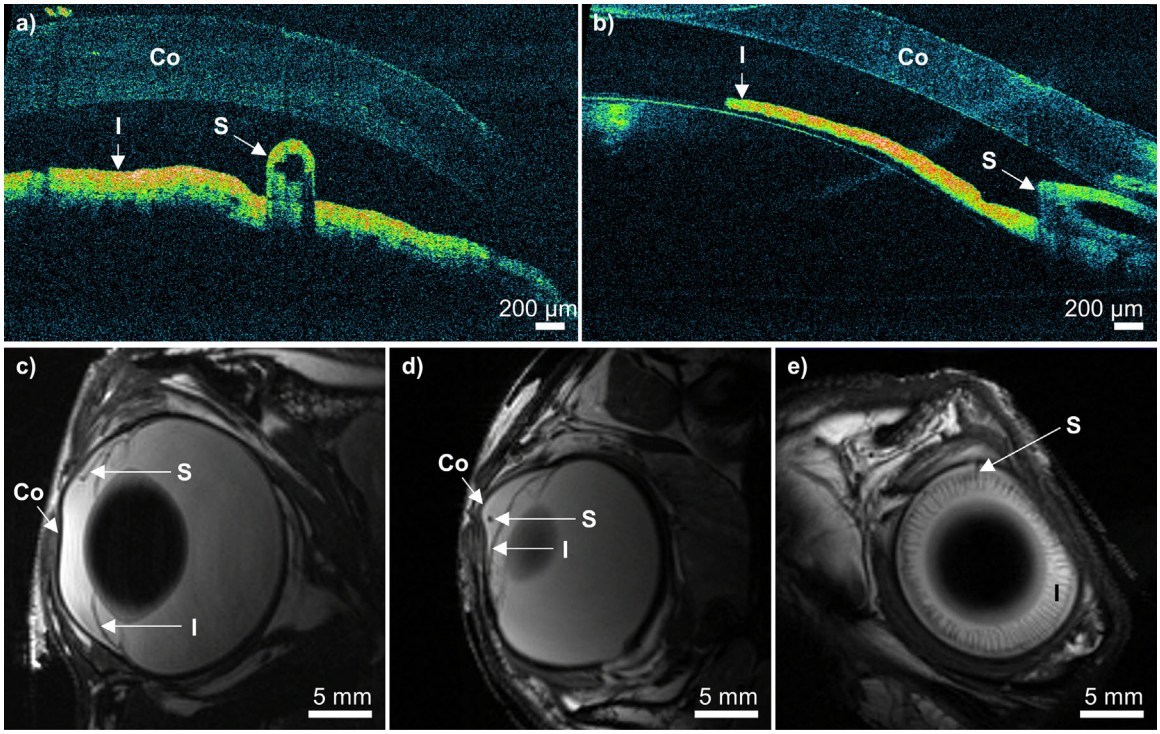

Figure 7. (a, b) Representative OCT imaging of an implanted microstent (S) inside the anterior chamber of a rabbit eye between cornea (Co) and iris (I): (a) longitudinal and (b) cross sectional imaging. (c–e) Representative ultrahigh field MRI of a rabbit eye implanted with a microstent: longitudinal (c), cross-sectional, (d) and frontal (e) views. An anatomically correct placement of the microstent inside the anterior chamber of the eye and inside the subconjunctival space was found.

The effects found during OPT remain equal throughout the whole 6-month (20-week) trial period, in group A and group B. IOP values recorded during OPT on right (treated) eyes and left (untreated) eyes (control eyes) 4, 8, 12, 16, and 20 weeks postoperatively are shown in Figure 6, for group A and group B.

Microstent Position Inside the Eye

Adequate microstent positioning inside the anterior chamber of a representative rabbit eye is shown in Figure 7a, b. The proximal microstent ending is located freely in the anterior chamber without any contact with the corneal endothelium. A representative ultrahigh field MRI of a microstent implanted into a rabbit eye is shown in Figure 7c–e. Adequate microstent positioning inside the anterior chamber of the eye and inside the subconjunctival space was found in all four animals of group A.

Discussion

MIGS currently represents a promising treatment approach for primary open-angle glaucoma. There are fundamental advantages of MIGS over conventional surgical glaucoma procedures: (i) the ab interno approach is based on a clear corneal incision without the need for a conjunctival perforation, (ii) the atraumatic procedure minimizes the operating field and therefore offers possibilities for a rapid patient recovery as well as for future surgical reinterventions, and (iii) there is a favorable safety profile. As soon as it will be possible to achieve a permanent drainage with MIGS, and thereby physiological IOP values, these procedures would be able to replace the classical and currently still considered gold standard surgical interventions such as trabeculectomy or deep sclerectomy, as well as conventional GDD. This factor emphasizes the clinical relevance and importance of MIGS. Nevertheless, commercially available devices such as the iStent, the iStent inject, or the XEN gel stent still do not represent a universally applicable safe solution for a long-term and effective IOP reduction.[2,7,18] In this regard, several studies reported remarkable hypotony rates after MIGS implantation. After CyPass implantation, hypotony rates ranging from 13.8% to 15.4% were reported.[7,10] In 9% of Xen gel stent implantations, patients needed a postoperative anterior chamber refill to stabilize IOP.[12] For the iStent, an incidence for

postoperative hypotension of 1% has been described in combined glaucoma and cataract surgery.[13] In case of the conventional GDD, Ahmed glaucoma valve 12% of the patients suffer from transient hypotony.[8]

Devices for the drainage of aqueous humor from the anterior chamber of the eye into the Schlemm's canal or into suprachoroidal space represent the most physiological approach with regard to natural fluid circulation inside the eye. Nevertheless, owing to a favorably high pressure difference between the anterior chamber and the subconjunctival space, devices draining into this area are most promising in the treatment of glaucoma. Because atmospheric pressure is present inside the subconjunctival space, the pressure difference to the anterior chamber corresponds with an IOP of 15.5 ± 2.8 mm Hg in healthy patients.[29] Nevertheless, bleb formation and fibrotic tissue reaction potentially add resistance to fluid drainage by decreasing the pressure difference. Therefore, antifibrotic microstent concepts represent a promising approach for an innovative device based MIGS. If the microstent tube were fully open, according to Hagen Poiseuille's law the expected volumetric flow rate extends the physiological aqueous humor production of approximately 2.5 µL min^{-1} by more than two orders of magnitude and, therefore, an ocular hypotony would be highly probable.[29,30] Considering ocular boundary conditions, the flow resistance of a constantly draining GDD should be approximately 6 mm Hg/µL min^{-1} (flow resistance = pressure difference/volume flow). For a need-based discontinuous drainage, a pressure adapted flow resistance of a GDD would be highly desirable. In this regard, different experimental valve mechanisms for GDD are described in literature.[30–34] Nevertheless, the surgically implanted Ahmed glaucoma valve currently represents the only commercially available valved GDD with a pressure dependent flow resistance ranging from 2.86 mm Hg/µL min^{-1} (valve closed) to 0.05 mm Hg/µL min^{-1} (valve opened).[35] Within the current work, we developed a pressure-controlled valve mechanism with a comparable flow resistance. We found a microstent flow resistance ranging from 2.65 ± 1.63 mm Hg/µL min^{-1} (valve closed) to 0.19 ± 0.05 mm Hg/µL min^{-1} (valve opened; $n = 4$). Therefore, the developed pressure-controlled valve represents an effective device for safe IOP regulation within physiological boundaries, that is, for the prevention of ocular hypotony.

Requirements for GDD can be found inside international standards and guidelines such as ANSI Z80.27-2014 or the 2015 US Food and Drug Administration guidance. Our in-house developed test setup for pressure flow characterization of GDD represents a further development of the previously described test setup now allowing for an online measurement over a broad range of pressure and volumetric flow rates.[19,36]

In addition to the adapted fluid mechanical properties of GDD, biocompatibility plays a key role. In this regard, polycarbonate urethanes represent a group of materials featuring excellent mechanical properties and biocompatibility that has resulted in a wide range of applications in the medical device segment.[37–41] Our study of the cytotoxicity of polycarbonate-based silicone elastomer using primary fibroblasts isolated from the human eye proved that this material is also suitable for ophthalmological applications. In addition, negative influences of microstent processing on cell viability could be excluded by the L929 eluate test on the prototypes (Supplementary Material S2).

As a consecutive step based on the in vitro experiments, in vivo animal experiments were carried out. IOP of rabbit eyes was analyzed as a major indicator of microstent safety and efficacy. Measurement of the IOP was conducted weekly on awake animals and monthly on anesthetized animals during OPT as a transient glaucoma model.[28] We observed a slightly decreased IOP in anesthetized rabbits compared with rabbits awake. This influence of general anesthetics on IOP has been described previously in the literature.[42,43] Thereby, the rebound tonometer used reaches its lower measurement range in anesthetized rabbit.

In general, microstent implantation results in a decrease in the IOP of treated right eyes versus left control eyes over the entire trial period of 6 months. In group A (microstents positionally stable), the IOP was decreased by approximately 10% in eyes implanted with a microstent compared with control eyes. The IOP in the eyes with implanted microstents was successfully regulated at approximately 12 mm Hg, close to the opening and closing pressure of the pressure-controlled valve. In group B (microstents migrated or dislocated) we found an IOP decrease of approximately 20% with IOP values of approximately 10 mm Hg in the treated eye. In case of group B, there was probably unregulated drainage through an undefined wound channel. No hypotony was found, either. In a clinical setting with glaucoma patients, the microstent offers perspectives for safe IOP regulation, whereas a wound channel remaining after microstent dislocation would probably lead to hypotension.

The current in vivo study was performed on healthy nonglaucomatous rabbits. Therefore, OPT was used as a transient glaucoma model. During OPT, there is an IOP decrease in untreated left eyes (control eyes) and in right eyes, implanted with a microstent. However, an IOP decrease is much more pronounced in eyes implanted with a microstent (group A). This positive effect persists throughout the entire 6-month

trial period and can be seen as an in vivo proof of concept for the microstent. In group B (microstents migrated or dislocated) a comparable effect was found, probably owing to drainage through the wound channel.

The developed MIGS procedure enables a safe microstent positioning inside the anterior chamber of the eye and inside the subconjunctival space, proven by means of in vivo imaging. No contact between microstents and the corneal endothelium was found within the current study, which has already led to the withdrawal of a MIGS implant from the market.[18] Our very flexible device adapts well to the curvature of the eyeball. Therefore, corneal endothelial cell loss is unlikely. Regardless, there is a risk of endothelial cell loss with any invasive operation on the eye. Therefore, endothelial cell count represents an important analysis for safety evaluation of novel GDDs and should be included in future studies.

The fixation of microstents in vivo represents a major limitation of the current study. Consequently, additional suture fixation was necessary for safe microstent placement. Commercially available devices for MIGS include various strategies for fixation. For example, the XEN Gel Stent fixates inside the MIGS wound channel by swelling of the device base material, cross-linked porcine gelatin, in the aqueous intraocular environment. Nevertheless, dislocation-associated complications cannot be completely avoided currently.[44] To avoid microstent dislocations in future studies, a limbal fixation mechanism that is compatible with our microstent and the applicator device is being developed currently.[45]

During the 21-week trial period, there were no noticeable changes in aqueous humor dynamics found in OPT measurements. Therefore, it is expected that there has been no marked fibrosis. Histological characterization of explanted eyes will give information on that in consecutive work. Nevertheless, it is known that fibrosis represents a major long-term complication in the clinical use of GDD.[7,46] For the prevention of fibrosis, cytostatic drugs such as mitomycin C or 5-fluorouracil are widely used in surgical glaucoma therapy but side effects of these unspecific agents are common.[47] Recent studies suggest, a positive effect of specific antifibrotic drugs such as PFD with regard to the prevention of fibrosis.[20,21] As an approved drug for human application, PFD represents a promising approach for glaucoma therapy.[48] Therefore, future in vivo studies will focus on the use of our drug-elutable microstent with the selectively antifibrotic drug PFD incorporated into its coating.[22]

Conclusions

The current preclinical study successfully provided a proof of concept for our novel valve-controlled microstent for MIGS. The microstent as well as the applied MIGS procedure are suitable for safe and effective IOP reduction. In contrast to commercially available devices for MIGS, safe IOP regulation within a physiological range is made possible. Furthermore, the future combination of the drug-elutable coating with a specific antifibrotic drug offers great potential for a long-term stable drainage efficiency in a clinical setting. The unique valve-controlled drug-elutable microstent offers promising perspectives for the clinical management of glaucoma as a novel treatment approach for MIGS.

Acknowledgments

The authors thank S. Grossmann and F. Kamke (Institute for ImplantTechnology and Biomaterials e.V., Rostock-Warnemünde, Germany) for the scanning electron microscopic examination and for support of pressure–flow characterization of microstents, respectively. The graphic support of A. Dierke (Institute for ImplantTechnology and Biomaterials e.V., Rostock-Warnemünde, Germany) in creating anatomic and technical illustrations (Figs. 1 and 2) is gratefully appreciated. Spray coating of microstents by D. Bajer is gratefully appreciated. The authors also thank the students J. Dostal, E. Fuhrmann, and J. Allahham for mechanical testing of the microstent material as well as the material modeling for the finite element analysis. The authors appreciate the excellent laboratory work as well as animal care of M. Nerger and G. Karsten (Institute for Biomedical Engineering, Rostock University Medical Center, Rostock, Germany), C. Leyh (Department of Ophthalmology, Rostock University Medical Center, Rostock, Germany), and P. Wolff (Institute for Experimental Surgery, Rostock University Medical Center, Rostock, Germany).

Financial support by the Federal Ministry of Education and Research within RESPONSE "Partnership for Innovation in Implant Technology" is gratefully acknowledged. The preclinical MRI system in the Core Facility Multimodal Small Animal Imaging was supported by European Regional Development Fund (EFRE funding: UHROM 16).

Author Contributions: S.S., M.S., W.S., R.G., and K.-P.S. developed the microstent concept. S.S.

conducted material testing of microstent base material and geometrical dimensioning of the pressure-controlled valve by means of finite element analysis. S.S. manufactured and processed microstents and applicator devices. U.H. and B.C. conducted manufacturing of flap valve mechanisms by means of fs-laser processing. S.S., M.S., and K.-P.S. developed a test setup for microfluidic characterization of the microstents and performed and interpreted in vitro pressure–flow characterization of microstent prototypes. S.S., S.K., N.G., R.G., K.-P.S., and T.S. conceived the concept of the preclinical in vivo study. R.G., T.S., S.K., and S.S. performed the in vivo experiments. R.G. performed all in vivo implantations as surgeon. L.L. and A.B. prepared and assisted during in vivo experiments. S.K., S.S., and T.S. performed analysis and interpretation of intraocular pressure measurements. S.K. and T.S. performed and analyzed OCT investigations. T.L. performed and analyzed MRI investigations. K.-P.S. and N.G. procured funding for the project. All authors reviewed the manuscript and approved the final version.

Ethics Approval Statement: Collection of donor material and its further use was approved by the ethics committee of the University of Rostock (approval ID: A2011 11) and followed the guidelines of the Declaration of Helsinki.

Disclosure: **S. Siewert**, None; **S. Kischkel**, None; **A. Brietzke**, None; **L. Kinzel**, None; **T. Lindner**, None; **U. Hinze**, None; **B. Chichkov**, None; **W. Schmidt**, None; **M. Stiehm**, None; **N. Grabow**, None; **R.F. Guthoff**, None; **K.-P. Schmitz**, None; **T. Stahnke**, None

[*] SS and SK contributed equally to this work.

References

1. Flaxman SR, Bourne RRA, Resnikoff S, et al. Global causes of blindness and distance vision impairment 1990-2020: a systematic review and meta-analysis. *Lancet Glob Health*. 2017;5(12):e1221–e1234.
2. Jonas JB, Aung T, Bourne RR, Bron AM, Ritch R, Panda-Jonas S. Glaucoma. *Lancet*. 2017;390(10108):2183–2193.
3. Diestelhorst M, Larsson LI, European-Canadian Latanoprost Fixed Combination Study Group. A 12-week, randomized, double-masked, multicenter study of the fixed combination of latanoprost and timolol in the evening versus the individual components. *Ophthalmology*. 2006;113(1):70–76.
4. Diestelhorst M. Medicinal therapy and course control of glaucoma. Options and limits of local therapy. *Der Ophthalmologe*. 2013;110(12):1132–1133.
5. Molteno AC. New implant for drainage in glaucoma. Animal trial. *Br J Ophthalmol*. 1969;53(3):161–168.
6. Lim KS, Allan BD, Lloyd AW, Muir A, Khaw PT. Glaucoma drainage devices; past, present, and future. *Br J Ophthalmol*. 1998;82(9):1083–1089.
7. Pillunat LE, Erb C, Jünemann AG, Kimmich F. Micro-invasive glaucoma surgery (MIGS): a review of surgical procedures using stents. *Clin Ophthalmol*. 2017;11:1583–1600.
8. Topouzis F, Coleman AL, Choplin N, et al. Follow-up of the original cohort with the Ahmed glaucoma valve implant. *Am J Ophthalmol*. 1999;128(2):198–204.
9. Gedde SJ, Schiffman JC, Feuer WJ, Herndon LW, Brandt JD, Budenz DL; Tube versus Trabeculectomy Study Group. Treatment outcomes in the Tube Versus Trabeculectomy (TVT) study after five years of follow-up. *Am J Ophthalmol*. 2012;153(5):789–803.e2.
10. Höh H, Grisanti S, Grisanti S, Rau M, Ianchulev S. Two-year clinical experience with the CyPass micro-stent: safety and surgical outcomes of a novel supraciliary micro-stent. *Klin Monbl Augenheilkd*. 2014;231(4):377–381.
11. Klewin DA, Dietlein TS, Haverkamp H. Glaucoma drainage devices - evaluation of surgical modifications to avoid postoperative complications. *Klin Monbl Augenheilkd*. 2020;237(11):1343–1352.
12. Sheybani A, Dick HB, Ahmed II. Early clinical results of a novel ab interno gel stent for the surgical treatment of open-angle glaucoma. *J Glaucoma*. 2016;25(7):e691–6.
13. Samuelson TW, Katz LJ, Wells JM, Duh YJ, Giamporcaro JE; US iStent Study Group. Randomized evaluation of the trabecular microbypass stent with phacoemulsification in patients with glaucoma and cataract. *Ophthalmology*. 2011;118(3):459–467.
14. Patel S, Pasquale LR. Glaucoma drainage devices: a review of the past, present, and future. *Semin Ophthalmol*. 2010;25(5-6):265–270.
15. Christakis PG, Kalenak JW, Tsai JC, et al. The Ahmed versus Baerveldt study: five-year treatment outcomes. *Ophthalmology*. 2016;123(10):2093–2102.
16. Mills RP, Reynolds A, Emond MJ, Barlow WE, Leen MM. Long-term survival of Molteno

glaucoma drainage devices. *Ophthalmology*. 1996;103(2):299–305.
17. Rotsos T, Tsioga A, Andreanos K, et al. Managing high risk glaucoma with the Ahmed valve implant: 20 years of experience. *Int J Ophthalmol.* 2018;11(2):240–244.
18. Fili S, Seddig S, Vastardis I, Perdikakis G, Wölfelschneider P, Kohlhaas M. Explantation of the CyPass implant in a case series of patients with corneal decompensation. *Der Ophthalmologe*. 2021;118(1):42–49.
19. Siewert S, Schultze C, Schmidt W, et al. Development of a micro-mechanical valve in a novel glaucoma implant. *Biomed Microdevices*. 2012;14(5):907–920.
20. Jung KI, Park CK. Pirfenidone inhibits fibrosis in foreign body reaction after glaucoma drainage device implantation. *Drug Des Devel Ther.* 2016;10:1477–1488.
21. Stahnke T, Siewert S, Reske T, et al. Development of a biodegradable antifibrotic local drug delivery system for glaucoma microstents. *Biosci Rep.* 2018;38(4):BSR20180628.
22. Siewert S, Reske T, Pfensig S, et al. Development of an antifibrotic drug-eluting coating for a minimally invasive implantable glaucoma microstent. *Curr Dir Biomed Eng.* 2019;5(1):215–218.
23. Siewert S, Schmidt W, Kohse S, et al. Development of a drug-eluting microstent for microinvasive glaucoma surgery. *Curr Dir Biomed Eng.* 2018;4(1):603–606.
24. Stahnke T, Löbler M, Kastner C, et al. Different fibroblast subpopulations of the eye: a therapeutic target to prevent postoperative fibrosis in glaucoma therapy. *Exp Eye Res.* 2012;100:88–97.
25. Löbler M, Rehmer A, Guthoff R, Martin H, Sternberg K, Stachs O. Suitability and calibration of a rebound tonometer to measure IOP in rabbit and pig eyes. *Vet Ophthalmol.* 2011;14(1):66–68.
26. Ulrich WD, Ulrich C. Oculo-oscillodynamography: a diagnostic procedure for recording ocular pulses and measuring retinal and ciliary arterial blood pressures. *Ophthalmic Res.* 1985;17(5):308–317.
27. Ulrich WD, Moeller A, Ulrich C, Siebert G, Wernecke KD, Erb C. Ocular blood flow regulation in glaucoma - examination with the ocular pressure flow analyzer (OPFA). *Klin Monbl Augenheilkd.* 2015;232(2):152–161.
28. Stahnke T, Siewert S, Walther E. Adopting oculopressure tonometry as a transient in vivo rabbit glaucoma model. *Curr Dir Biomed.* 2015;1(1):127–130.
29. Collins R, Van der Werff TJ. Mathematical models of the dynamics of the human eye. *Lecture notes in biomathematics, Band 34*. Berlin, Heidelberg: Springer-Verlag; 1980.
30. Park CJ, Yang DS, Cha JJ, Lee JH. Polymeric check valve with an elevated pedestal for precise cracking pressure in a glaucoma drainage device. *Biomed Microdevices*. 2016;18(1):20.
31. Kara E, Kutlar AI. CFD analysis of the Ahmed glaucoma valve and design of an alternative device. *Comput Methods Biomech Biomed Engin.* 2010;13(6):655–662.
32. Moon S, Im S, An J, et al. Selectively bonded polymeric glaucoma drainage device for reliable regulation of intraocular pressure. *Biomed Microdevices*. 2012;14(2):325–335.
33. Paschalis EI, Chodosh J, Sperling RA, Salvador-Culla B, Dohlman C. A novel implantable glaucoma valve using ferrofluid. *PloS One*. 2013;8(6):e67404.
34. Schwerk B, Harder L, Windhövel C, et al. Comparison of two prototypes of a magnetically adjustable glaucoma implant in rabbits. *PloS One*. 2019;14(4):e0215316.
35. Prata JA, Jr, Mérmoud A, LaBree L, Minckler DS. In vitro and in vivo flow characteristics of glaucoma drainage implants. *Ophthalmology*. 1995;102(6):894–904.
36. Turhan S, Kara E, Kutlar A, Güngör KA. Short survey on currently used experimental setups for testing glaucoma drainage devices. *Eur Mech Sci.* 2018;2(2):60–67.
37. Gooch N, Burr RM, Holt DJ, Gale B, Ambati B. Design and in vitro biocompatibility of a novel ocular drug delivery device. *J Funct Biomater.* 2013;4(1):14–26.
38. Sheikhhassani R, Anvari P, Taei S, Sheikhhassani Y. Potential use of a polycarbonate-urethane matrix reinforced with polyethylene fibers for shock-absorbing dental implants. *Med Hypotheses*. 2015;85(3):241–244.
39. Zhu R, Wang Y, Zhang Z, Ma D, Wang X. Synthesis of polycarbonate urethane elastomers and effects of the chemical structures on their thermal, mechanical and biocompatibility properties. *Heliyon*. 2016;2(6):e00125.
40. Eilenberg M, Enayati M, Ehebruster D, et al. Long term evaluation of nanofibrous, bioabsorbable polycarbonate urethane grafts for small diameter vessel replacement in rodents. *Eur J Vasc Endovasc Surg.* 2020;59(4):643–652.
41. Pritchett JW. Total articular knee replacement using polyurethane. *J Knee Surg.* 2020;33(3):242–246.

42. Chae JJ, Prausnitz MR, Ethier CR. Effects of general anesthesia on intraocular pressure in rabbits. *J Am Assoc Lab Anim Sci*. 2021;60(1):91–95.
43. Jantzen JP. Anesthesia and intraocular pressure. *Anaesthesist*. 1988;37(8):458–469.
44. Fea AM, Bron AM, Economou MA, et al. European study of the efficacy of a cross-linked gel stent for the treatment of glaucoma. *J Cataract Refract Surg.* 2020;46(3):441–450.
45. Siewert S, Großmann S, Brandt-Wunderlich C, et al. Development of a limbal fixation mechanism for a minimally invasive implantable glaucoma microstent. *Curr Dir Biomed Eng.* 2020;6(3):20203056.
46. Dietlein TS, Jordan J, Lueke C, Krieglstein GK. Modern concepts in antiglaucomatous implant surgery. *Graefes Arch Clin Exp Ophthalmol.* 2008;246(12):1653–1664.
47. Mostafaei A. Augmenting trabeculectomy in glaucoma with subconjunctival mitomycin C versus subconjunctival 5-fluorouracil: a randomized clinical trial. *Clin Ophthalmol.* 2011;5:491–494.
48. Hilberg O, Simonsen U, du Bois R, Bendstrup E. Pirfenidone: significant treatment effects in idiopathic pulmonary fibrosis. *Clin Respir J.* 2012;6(3):131–143.